Attitude and Altitude Estimation and Control on board a Flapping Wing Micro Air Vehicle

J.L. Verboom[1], S. Tijmons[2], C. De Wagter[2], B. Remes[2], R. Babuska[1], G.C.H.E. de Croon[2]

***Abstract*— The autonomous capabilities of light-weight Flapping Wing Micro Air Vehicles (FWMAVs) have much to gain from onboard state estimation and attitude control. In this article, we present the first FWMAV with *robust* onboard state estimation and attitude control. The tailed FWMAV DelFly II was used, with the main goal to achieve active stabilization in the (passively unstable) hover condition. The attitude is estimated using an Inertial Measurement Unit with a gyroscope, accelerometer and magnetometer and the altitude is estimated using a barometer. A major challenge lies in the disturbance of the accelerometer measurements by the flapping motion of the wings. We propose a mechanical damping mechanism and flap-cycle based filtering to resolve this issue. The pitch estimates have a mean error of 1.5° with respect to the ground-truth measurement from a motion capture system. Using the onboard pitch estimate we can control the attitude of the FWMAV in the forward flight regime with a 30% lower standard deviation than in a trimmed flight. With a different set of gains, the FWMAV is able to perform a hovering flight - showing that a tailed FWMAV has enough control authority for this task. In a fully autonomous hover experiment, the DelFly II stays within a sphere of 0.75 m radius.**

I. INTRODUCTION

The field of Flapping Wing Micro Air Vehicles (FWMAVs) presents many technological challenges, exacerbated by the small sizes of the vehicles, which impose constraints on the onboard components. It is already challenging to achieve flight with an FWMAV, so the focus is typically still more on design, rather than on autonomous flight capabilities such as onboard state estimation and control. A major subdivision of FWMAVs can be made according to the presence or absence of a stabilizing tail. Tailless designs, such as [1], [2], control their attitude by varying wing stroke parameters. These designs are inherently unstable and require active attitude stabilization for achieving stable flight (manual or autonomous).

Tailed designs such as [3], [4] are passively stable given a minimal forward velocity. However, this has an influence on the maneuverability as it induces a minimum turn radius. In small confined spaces this is a problem as it limits the set of possible trajectories which can be safely undertaken and complicates the required obstacle avoidance strategies (cf. [5]). If an FWMAV has the ability to minimize the forward velocity or even hover, the navigation in small confined spaces would be significantly improved.

The passive stabilization of a tailed FWMAV is achieved by the tail section, which behaves as a natural damper on the system. It dampens out the oscillations induced by the motion of the flapping wings. During forward flight the air flow over the control surface consists of two components: the airflow due to spatial movement of the ornithopter and the airflow induced by the flapping of the wings. During hovering the former airflow is not present and the system is no longer passively stabilized by the tail section. It is unclear if the control surfaces are sufficiently fast and strong to autonomously control the FWMAV near hover.

In order to achieve active attitude stabilization, sensing and control of the state is required. Although this can be achieved with external systems [6], [7], for real-world operation it is far preferable to have an onboard solution. The first attempt to increase the stability of an FWMAV with onboard sensors [1] featured a gyroscope for feedback rotation rate stabilization of a further manually controlled tailless FWMAV. Alternatively, the gyroscope has been integrated for state estimation and attitude control for relatively short time spans [3], [9]. Due to the inherent bias of a gyroscope it cannot be robustly and solely used for attitude estimation and control. The first attempt to perform absolute attitude estimation and control for an FWMAV featured a magnetometer [10]. The selection of the magnetometer is advantageous as it is undisturbed by the mechanical vibrations, in contrast to an accelerometer. However, the measurements from a magnetometer may vary due to environmental disturbances.

In order to achieve long term attitude control, robust state estimation is required. This may be achieved by fusion of multiple sensors such as gyros and accelerometers. However, the flapping wing movements heavily perturb the accelerometer measurements. For instance, on the tiny Robobee [9] it was observed that the flapping caused accelerations in the range ± 5 g. The accelerometer measurements had a distortion of -2m/s^2, which was larger than the accelerations of interest, in the order of 1m/s^2.

In this article, we present the first robust onboard state estimation and control on board of a light-weight FWMAV. Our main contributions are: (1) methods to filter the accelerometer measurements for use in onboard attitude estimation, (2) an efficient onboard state estimator and (3) a control scheme which improves the autonomous capabilities of an FWMAV platform. In Section II, we explain the DelFly II — the platform used for the experiments. In Section III we explain the onboard sensors. Then, in Section IV and V we present the efficient state estimation and control algorithms running on board of the ATmega328P microprocessor. In Section VI, results of flight experiments are presented. Finally, conclusions are drawn in Section VII.

[1] Delft Center for Systems and Control, Faculty of Mechanical Engineering and Systems, Delft University of Technology

[2] Micro Air Vehicle laboratory, Faculty of Aerospace Engineering, Delft University of Technology microuav@gmail.com

II. THE DELFLY II

The DelFly has been under continuous development and has improved in a variety of aspects, including lift generation, the onboard hardware and its autonomous capabilities [4]. Only recently, the newest version of the DelFly was presented, the DelFly Explorer [8], which achieved autonomous flight and obstacle avoidance using a stereo vision camera module. All computations are performed on board the DelFly Explorer. The autonomous flight was achieved in a trimmed slow forward flight condition. In principle there is no requirement to do onboard state estimation and control, as the DelFly is an intrinsically stable platform in this slow forward flight regime ($\sim 1m/s$). However, the hover capability would significantly simplify and improve the DelFly's obstacle avoidance performance, as obstacles then would not have to be detected as far away as it currently is the case (around 3 m ahead). During hovering, the DelFly is no longer passively stabilized by the tail section and thus becomes unstable. Additionally, the position of the center of mass is important as it balances the forces and moments between the wings and the tail section.

The current configuration of the DelFly is shown in Figure 1a and the definition of the body-frame axes in Figure 1b. The DelFly has four actuators: a brushless DC motor for controlling the flapping frequency of the double wing pairs and three servos. The DC motor runs at a frequency of around 320 Hz, and after a transmission (21.3 : 1) this results in a flap frequency of about 15 Hz. One servo is used to actuate the ailerons that are positioned close behind the wings (roll control), and two servos actuate the rudder and elevator surfaces on the tail (yaw and pitch control).

The DelFly hosts an autopilot board of 0.9 gram. The autopilot board contains the ATmega328P micro-processor, the BMP-180 barometric pressure sensor and the MPU9150 9-axis IMU with an accelerometers, gyroscopes and magnetometers. Additionally, a transceiver is present for remote controlled flight and telemetry. An extra magnetometer was added because the magnetometer on the IMU chip did not work robustly during tests. The extra sensor, the HMC5883L, has the benefit that it is more accurate and that it can sample at a higher frequency, while adding only 0.1 gram extra weight. All the components and the sensors used are discussed in further detail in the next section. Furthermore, in order to validate the onboard estimates of the attitude in a motion tracking arena, small reflective markers are attached to various surfaces on the DelFly.

III. ONBOARD SENSORS

An overview of all the onboard sensors with their key specifications is given in Table I.

TABLE I: Characteristics of the onboard sensors

Characteristic	Frequency	Output range	Sensitivity
Accelerometer	1 kHz	± 16 g	2,048 LSB/g
Gyroscope	8 kHz	$\pm 2000^\circ/s$	16.4 LSB/($^\circ/s$)
Magnetometer	75 Hz	± 4.7Ga	2.56 mGa/LSB
Barometer	128 Hz	300 - 1100 hPa	0.01 hPa/LSB

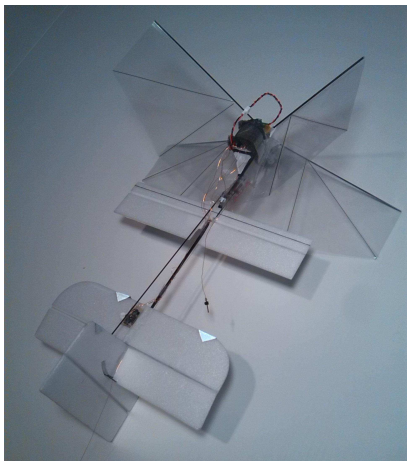

(a) The DelFly II during hovering

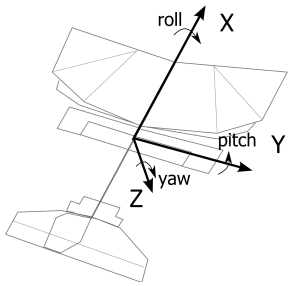

(b) The DelFly II body-frame axes definition

Fig. 1: The DelFly II platform

A. Inertial Measurement Unit

The accelerometer and gyroscope both have 3 axes/channels that provide a 16-bit digital output. The measurements are stored in a FIFO buffer which is part of the sensor; by using the FIFO buffer, the sensor can sample at a higher frequency ($615Hz$) relative to the loop frequency of the attitude loop on the CPU ($\sim 100Hz$).

The magnetometer is able to measure the magnetic field along the three principal axes of the sensor. The magnetometer is calibrated for the hard-iron offset and corrected for the onboard induced magnetic field which is dominated by the motor.

B. Barometer

The digital barometric pressure sensor is the BMP-180 sensor and it features a static pressure sensor and temperature sensor. The measured pressure is internally corrected for the ambient temperature. The characteristic RMS of the noise of the sensor is 0.03 hPa, which is equivalent to 0.25 m at sea level.

C. Sensor Attachment

In order to cope with high frequency vibrations, the autopilot board is placed inside a foamy substructure as shown in Figure 2. This method of attachment of the autopilot board

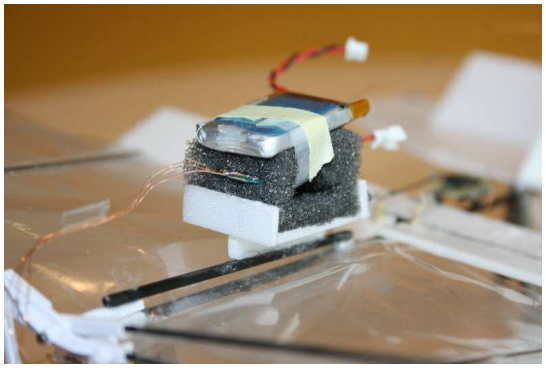

Fig. 2: The autopilot board placement with the battery. The battery is placed on top of the foam and attached to the foam using tape. The autopilot board is wedged in the foam and can be observed in the front where the wires exit the foam.

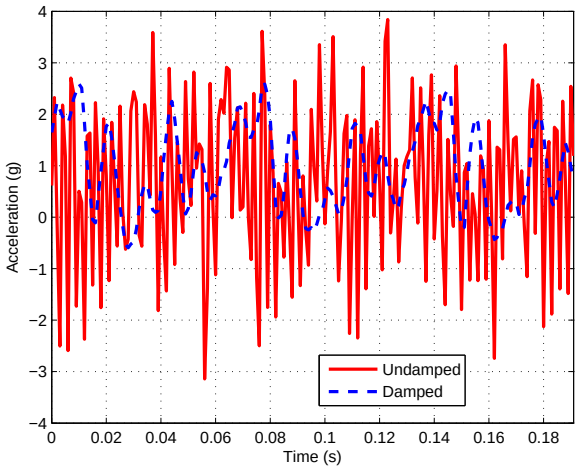

Fig. 3: The effect of mechanically damping the autopilot board. The results show the X-axis accelerometer measurements for the undamped and the damped system at a large pitch angle ($\sim 80°$).

was chosen such that any high frequency disturbances from the motor are mechanically damped. As can be seen in the figure, the battery is firmly attached to the isolated autopilot board. By including the mass of the battery (at least $3.5g$), the natural frequency of the autopilot/battery combination is low enough ($< 100Hz$) to be measured and filtered.

The effect of the foamy substructure on the measurements of the accelerometer was evaluated by performing two tests: one test where the autopilot board is directly attached to the airframe (undamped - red line) and one test where the autopilot is placed inside the foamy substructure (damped - blue dotted line) as in the figure. The accelerometer measurements were conducted during flight at a large pitch angle ($\sim 80°$) and at a sampling frequency of 1 kHz. Figure 3 shows that the undamped measurements of the accelerometer are dominated by high frequency vibrations that are induced by the DC motor. The vibrations produced by the motor (which runs at $\sim 300Hz$) and its harmonics turned out to be higher than the Nyquist frequency. The measurements obtained from the damped system show much smoother and repetitve vibrations which are caused by the periodic motion of the wings. These vibrations contain frequencies that can be filtered as is discussed in the next section.

IV. STATE ESTIMATION

The attitude is represented by the three Euler angles: roll (ϕ), pitch (θ) and yaw (ψ). The accelerometer measurement $\mathbf{a} = [a_x, a_y, a_z]^T$ is used to estimate the roll and pitch angles; the magnetometer measurement $\mathbf{m} = [m_x, m_y, m_z]^T$ is used to estimate the yaw angle. For the definition of the Euler angles, the $2-1-3$ rotation sequence (pitch-roll-yaw) is used. The angles are defined as:

$$\begin{aligned} \widetilde{\theta} &= atan(\tfrac{-a_x}{a_z}) \\ \widetilde{\phi} &= atan(\tfrac{-a_y}{\sqrt{a_x^2+a_z^2}}) \\ \widetilde{\psi} &= atan(\tfrac{\sin(\phi)\sin(\theta)m_x+\cos(\phi)m_y+\sin(\phi)\cos(\phi)m_z}{\cos(\theta)m_x+\sin(\theta)m_z}) \end{aligned} \quad (1)$$

This definition of the Euler angles ensures that the pitch angle is defined also for high pitch angles ($> 90°$) that occur during hover. This is a benefit when compared to the more general $1-2-3$ rotation sequence (roll-pitch-yaw). Furthermore, the chosen rotation sequence also leads to more stable estimations of the roll and pitch angle. The reason for this is that the DelFly (normally) flies with small roll angles, which means that the gravitational force is expected to be predominately present on the X and Z body axes (and the same accelerometer axes). From Equation 1 it can be seen that the roll and pitch angle can therefore be robustly measured.

In order to compute the Euler angles correctly: the $atan$, $\sin$ and $\cos$ functions are required on board. A library is preferably not included, because of memory constraints of the micro-controller; therefore the CORDIC algorithm [11] is used on board to calculate all the necessary trigonometric functions.

The implicit assumption from Equation 1 is that the accelerometer measurements are only influenced by the gravitational force. From the measurements in Figure 3, this is known to be untrue; additional filtering and fusion steps are required in order to perform onboard state estimation. This will be discussed in the two following subsections.

A. Accelerometer data filtering

The accelerometer measurements are disturbed by a constant periodic motion: the flapping of the wings. The measurements are therefore filtered using a moving average filter. The moving average filter can be implemented and adopted efficiently on board and the output of the filter will be an unbiased component of the gravitational force. The length of the moving average filter is based on the measured motor frequency. Filtering the measurements of the accelerometer with such a moving average filter serves two purposes:

- The output of the moving average filter - based on the flap cycle - is an unbiased measurement of the

gravitational force,
- The previous statement is valid for all flapping frequencies and all pitch angles.

The stability of the accelerometer measurements for a series of different lengths of the moving average filter is shown in Figure 4. The figure shows the signal-to-noise ratio for different lengths of the moving average filter.

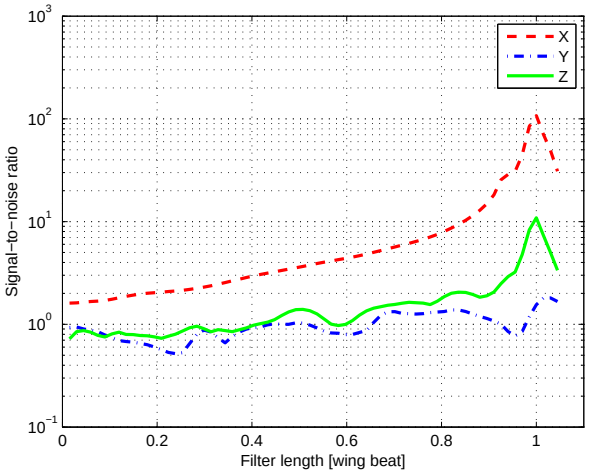

Fig. 4: The signal-to-noise ratio of the accelerometer measurements as a function of the filter length expressed as unit of wing beat.

The signal-to-noise ratio of the filtered measurements increases sharply as the length of the filter approaches the length of the wing beat cycle. As the length of the filter exceeds the length of the wing beat cycle the signal-to-noise ratio again deteriorates. Filtering the accelerometer measurements based on the wing beat cycle while using a moving average filter results in a robust estimate of the gravitational force.

B. Accelerometer and gyroscope fusion

The moving average filter results in smoother accelerometer measurements that enhance the roll and pitch angle estimates. These estimates can be further improved by using the gyroscope measurements $\mathbf{g} = [g_x, g_y, g_z]^T$. To combine the measurements from the accelerometers with those from the gyroscope a first-order complementary filter is used. The function of the filter for the pitch angle is given by:

$$\hat{\theta}_k = (1-\tau)\widetilde{\theta} + \tau(\hat{\theta}_{k-1} + g_y \Delta t) \qquad (2)$$

where $\hat{\theta}_k$ is the pitch estimate at the current time k, $\widetilde{\theta}$ is the measured pitch angle based on Equation 1, Δt is the time step and τ is a weight factor which is set at 0.9. The roll and yaw angle are filtered in the same way using their corresponding gyroscope measurements.

C. Altitude estimation

The atmospheric pressure measurements from the barometer are filtered using a first-order low-pass filter; the filter is given by the following function:

$$\hat{h}_k = \hat{h}_{k-1} + (\widetilde{h} - \hat{h}_{k-1})G \qquad (3)$$

In this equation $\hat{h}_k$ is the current estimate of the atmospheric pressure and $\widetilde{h}$ is the new measurement from the barometer. G is a gain factor which is set at 0.1 such that the noisy barometer measurements are significantly smoothed.

V. CONTROL DESIGN

For the control strategy of the DelFly a distinction is made between forward flight and hovering flight. In order to stabilize the DelFly in forward flight the longitudinal controller is used; while in the hovering flight regime the lateral, longitudinal and altitude controllers are used. In hovering flight the DelFly is unstable and all these control loops are required in order to stabilize the attitude and altitude. All controllers are PID controllers.

The gains of the forward flight controller have been tuned using the Ziegler-Nichols method [12] and all the gains for the hovering flight controller are experimentally tuned.

A. Forward flight controller

A closed-loop controller is used to improve the stability and control accuracy of the forward flight regime of the DelFly. Longitudinal control is achieved by the elevator. For forward flight a desired attitude is selected for the pitch angle, which can range from 60 to 80 degrees.

B. Hovering flight controller

During hovering the passive stability induced by the tail section is lost and the DelFly is unstable. In the hovering flight regime the attitude is actively controlled; the elevator is used for longitudinal control and the ailerons and rudder for lateral control. During hovering, the thrust vector points straight down and no additional lift is generated from the wings or other control surfaces. The small deflections of the control surfaces cause drag, and this has an effect on the altitude. Therefore the altitude also needs to be actively controlled.

The attitude is controlled using three separate controllers: a PID controller on the elevator for the pitch angle, a PD controller on the rudder for yaw control, and a PD controller on the ailerons for heading control. It is critical for hovering to correctly stabilize the pitch angle because any deviation will result in a positive or negative forward flight speed. The yaw and pitch angles need to be damped and corrected for, but these angles are less critical.

The altitude controller drives the DC motor and features two different feedback loops. The inner loop controls the velocity of the DC motor. The motor frequency is measured and controlled using a PID controller. The outer loop controls the altitude using the measurements from the barometer. The altitude controller is a PI controller around a fixed reference pressure which is set before the flight based on the current atmospheric conditions.

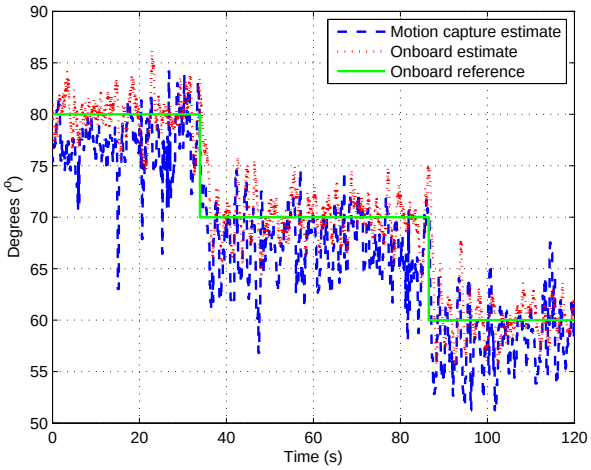

Fig. 5: The pitch angle during the first forward flight experiment. The signal in red is the onboard estimate of the pitch angle, and the green signal is the reference value of the pitch angle. The measurement from the motion tracking arena is depicted in blue.

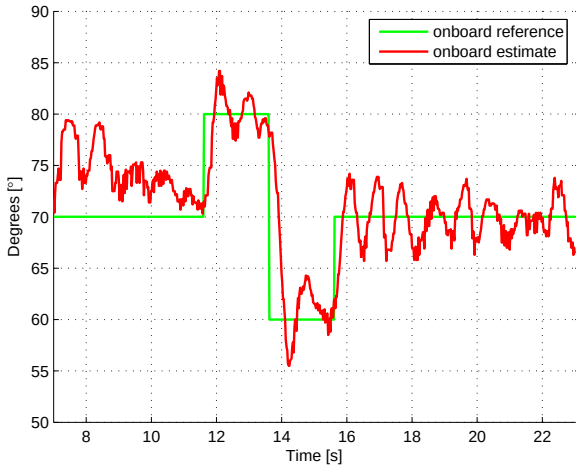

Fig. 6: The pitch angle during the second forward flight experiment. The reference pitch angle (green) forms a doublet with intervals of two seconds, the red line shows the pitch angle of the DelFly as measured on board.

VI. EXPERIMENTS

The onboard estimates of the DelFly are validated in a motion tracking arena, with an area of 4 square meter and 6 active cameras. The motion of the DelFly is tracked using small reflective markers, which are used to determine the attitude and position. To illustrate the difference between the two flight regimes, the gains of the longitudinal controller for both the regimes are shown in table II.

PID gains	K_p	K_i	K_d
Forward flight	0.25	1.688	0.000044
Hovering flight	0.25	1.125	0.000350

TABLE II: The gains of the longitudinal controller for the two different flight regimes.

The difference between the two gain sets is significant and the K_d gain in hovering flight is 8 times larger than the K_d in forward flight. The loss of the passive damping effect from the tail explains the higher value of K_d. Furthermore, the K_i and K_p gains are considerably larger than the K_d gain for both the hovering and forward flight regime.

A. Forward flight

Experimental results from the onboard estimator and forward flight controller are shown in Figure 5. The forward flight controller is tested for three different reference angles: 80, 70 and 60 degrees. The results are achieved using a single set of controller gains which yield similar results across the domain of the pitch angle.

The RMSE in degrees of the onboard estimate versus the reference is determined for the three different intervals of the forward flight controller.

$$\begin{aligned} \text{RMSE}_{80} &= 2.0618^\circ \\ \text{RMSE}_{70} &= 2.0626^\circ \\ \text{RMSE}_{60} &= 2.0077^\circ \end{aligned}$$

The performance of the controller versus the trimmed flight condition is significantly higher. Typically, the standard deviation during free flight of the DelFly is on the order of $\sigma_{ff} = 6^\circ$, while the standard deviation of the pitch angle during controlled forward flight is $\sigma_{cf} = 4^\circ$. The longitudinal flight controller results in a 30 $\%$ decrease in the standard deviation of the pitch angle and the estimate has a mean error of 1.5° with respect to measurements from the motion capture arena. Figure 6 shows results from a test with a doublet input on the pitch reference signal. The same values for the reference angles were chosen as in the first test. The results show a response time of around 200ms but also a significant overshoot and a slowly damped pitch oscillation.

B. Hovering flight

In the hovering flight regime the DelFly is solely controlled by the different control loops to stabilize the attitude and altitude, and as a consequence the DelFly maintains its spatial position if it operates in an area without any airflow disturbances. The control variables are the pitch, yaw, roll and altitude and are respectively controlled by the elevator, ailerons, rudder and DC motor. The first experiment lasts more than 40 seconds and in that time the autopilot is able to stabilize the DelFly. The reference angle is set to 90.5°; this reference value was chosen experimentally, such that the forward velocity is zero. The RMSE of the pitch angle of the onboard estimate versus the reference angle for the hovering experiment is:

$$\text{RMSE} = 4.0817^\circ$$

The hover regime is important to autonomous flight, since it should allow the DelFly to remain spatially stable (in the absence of airflow disturbances). Therefore, the spatial position of the DelFly during hover is analyzed. The position during the hovering experiments is shown in figure 7. The results show the DelFly is able to maintain its position on the ground surface within a circle with a radius of 0.75 meter. Videos of several test flights can be found on the website of the DelFly project[1].

Figure 8 shows the onboard estimates of the roll, pitch and yaw angles during a hover flight. The results show that the controllers are able to track the reference roll and pitch angle, but that the yaw angle is quite off. This is caused by the fact that the effectiveness of the aileron surfaces becomes very poor at zero speed.

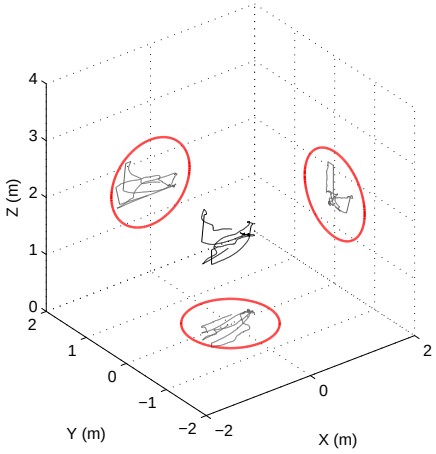

Fig. 7: The spatial position of the DelFly during hovering. In black is the actual spatial position and the measurements in gray are the projections of the measurement. A circle with a radius of 0.75 meter is projected on the ground surface to indicate the performance of the hovering flight controller in the absence of wind.

VII. CONCLUSIONS

For the fist time robust onboard state estimation and control of the attitude and altitude of a tailed light-weight FWMAV is achieved.

It is shown that a mechanical damping solution results in useful accelerometer measurements without undersampling issues. The flap-cycle moving average filter for the accelerometer greatly improves the signal-to-noise ratio of the measurements. The filter proves to produce accurate attitude estimates: the pitch estimates have a mean error of $1.5°$ with respect to measurements from the motion capture arena. Attitude control is achieved using PID controllers. The application of the controller to the forward flight regime resulted in a standard deviation of the pitch angle which was 30% lower than for trimmed flight. The hovering flight

[1] `http://www.delfly.nl/ICRA2015.html`

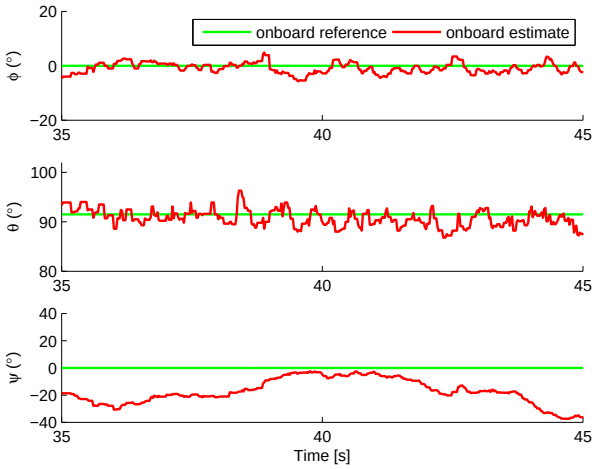

Fig. 8: Estimates of the roll, pitch and yaw angles from the onboard sensors during hover flight.

controller features different control loops for the pitch, roll and yaw angles and the altitude. The tailed FWMAV is able to hover, with a performance which is slightly less than for the forward flight controller. During the hovering experiment, the spatial movement is limited to a sphere with a radius of 0.75 meter.

REFERENCES

[1] Keennon, Matthew, et al. "Development of the nano hummingbird: A tailless flapping wing micro air vehicle." AIAA Aerospace Sciences Meeting. 2012.

[2] Ma, Kevin Y., et al. "Controlled flight of a biologically inspired, insect-scale robot." Science 340.6132 (2013): 603-607.

[3] Baek, Stanley S., Fernando L. Garcia Bermudez, and Ronald S. Fearing. "Flight control for target seeking by 13 gram ornithopter." Intelligent Robots and Systems (IROS), 2011 IEEE/RSJ International Conference on. IEEE, 2011.

[4] De Croon, G. C. H. E., et al. "Design, aerodynamics, and vision-based control of the DelFly." International Journal of Micro Air Vehicles 1.2 (2009): 71-97.

[5] Tijmons, S., de Croon, G.C.H.E., Remes, B.D.W., De Wagter, C., Ruijsink, R., Van Kampen, E-J, Chu, Q., "Stereo Vision Based Obstacle Avoidance on Flapping Wing MAVs", EuroGNC 2013, Delft, (2013).

[6] Ma, K. Y. , Chirarattananon, P. , Fuller, S.B. and Wood, R.J. "Controlled flight of a biologically inspired, insect-scale robot", Science, 340(6132):603607, 2013.

[7] Hsiao, F. Y., H. K. Hsu, C. L. Chen, L. J. Yang, and J. F. Shen. "Using stereo vision to acquire the flight information of flapping-wing MAVs." Journal of Applied Science and Engineering 15, no. 3 (2012): 213-226.

[8] De Wagter, Christophe, et al. "Autonomous flight of a 20-gram flapping wing mav with a 4-gram onboard stereo vision system." Proc. 2014 IEEE/RSJ Int. Conf. on Robotics and Autonomous Systems (ICRA), Hong Kong, China, 25 June 2014. 2014.

[9] Fuller, Sawyer B., et al. "Using a MEMS gyroscope to stabilize the attitude of a fly-sized hovering robot." IMAV 2014: International Micro Air Vehicle Conference and Competition 2014, Delft, The Netherlands, August 12-15, 2014. Delft University of Technology, 2014.

[10] Helbling, Elizabeth Farrell Fuller S. Wood R. "Pitch and Yaw Control of a Robotic Insect Using an Onboard Magnetometer"

[11] Volder, Jack E. "The CORDIC trigonometric computing technique." Electronic Computers, IRE Transactions on 3 (1959): 330-334.

[12] Ziegler, J. G., and N. B. Nichols. "Optimum settings for automatic controllers." trans. ASME 64.11 (1942).